

Miniband dispersion in (In,Ga)As-GaAs strained-layer superlattices

Karen J. Moore, Geoffrey Duggan, Age Raukema,* and Karl Woodbridge

Philips Research Laboratories, Redhill, Surrey RH1 5HA, England

(Received 16 February 1990)

Photoluminescence excitation (PLE) spectroscopy has been used to characterize miniband formation in (In,Ga)As-GaAs superlattices with nominally 50-Å-wide wells and barriers between 50 and 200 Å. The nominal composition of the alloy layers was ~ 0.06 . The observed exciton features are consistent with theoretical predictions of the $\Delta n = 0$ and $\Delta n \neq 0$ (i.e., $e1$ -hh2) intersubband transitions both at the center of the superlattice minizone and at the zone edge. The observation of these features allows us to map the evolution of the superlattice minibands at energies both above and below the top of the superlattice potential, with decreasing barrier thickness. Furthermore, as the GaAs thickness is varied, a dramatic change in shape of PLE spectra occurs in the region of the first free-electron-to-heavy-hole subband continuum. For samples in which the electron miniband width is comparable with the exciton binding energy, a significant enhancement of the absorption strength is observed, brought about by a redistribution of the oscillator strengths of the continuum states due to the electron-hole, Coulomb interaction. The best agreement with the measured exciton positions is found using a band-offset ratio of $\sim 67:33$.

INTRODUCTION

The transition from a multiple-quantum-well structure to a real superlattice (SL) occurs when the barriers between quantum wells become sufficiently thin that the eigenfunctions of the individual wells hybridize, forming minibands with finite energy widths.^{1,2} The width, or energy dispersion, of the minibands can be varied by changing sample parameters; for example, an increase in band width is achieved by either decreasing the barrier thickness for a fixed well width, or decreasing the well thickness at a fixed barrier thickness.^{3,4} The periodic one-dimensional (1 D) SL potential (of depth V , say) also produces subbands above the barriers, separated by forbidden energy gaps. These subbands show similar miniband dispersion that also depends on the barrier thickness. We refer to the electronic states above the barrier, with energies $> V$, as unconfined states, while those within the quantum wells, with energies $< V$, are "confined" states which can be either localized (as in isolated quantum-well structures) or delocalized, if the barriers are thin.

As a result of the energy subband dispersion in the superlattice band structure along q_z , the wave vector in the sample growth direction, M_1 -type critical points (saddle points) are formed at the 1D Brillouin-zone boundary.⁵⁻⁷ The effects of this additional critical point in the band structure on the absorption spectra of superlattice structures has been investigated theoretically by Chu and Chang.⁸ Their calculations, which take into account the Coulomb interaction between electrons and holes within the miniband, demonstrate that there can be a significant modification of the shape of the absorption spectrum, particularly when the electron bandwidth is of the order of the heavy-hole exciton binding energy. More recently, features in the PLE spectra of GaAs-(Al,Ga)As superlattices⁹⁻¹¹ related to the miniband dispersion along q_z and the presence of the M_1 -type critical point at the minizone

boundary in the energy band structure, have been reported. Magneto-optic measurements^{9,11} have shown these features, which are characterized by their rather broad shape (in contrast to the much sharper exciton peaks associated with the M_0 critical point) to be excitonic in origin.

We report optical investigations of excitons associated with the formation of minibands in (In,Ga)As-GaAs strained-layer superlattice structures, where the indium fraction in the alloy layers is nominally 0.06. By keeping the (In,Ga)As layer thickness fixed, and adjusting the GaAs barrier thickness between samples, we have varied the $n = 1$ electron miniband width from approximately 2 up to 43 meV. Our photoluminescence excitation (PLE) measurements reveal sharp excitonic resonances, associated with both the lowest and higher subbands, which we are able to follow as a function of the barrier thickness. We compare the measured exciton positions with Kronig-Penney "envelope-function"-type calculations.

There are a number of advantages associated with investigating miniband formation in the strained (In,Ga)As-GaAs material system over the more commonly studied GaAs-(Al,Ga)As superlattices. For example, the presence of strain in the alloy layers produces a significant increase in the heavy-hole to light-hole splitting, allowing features in the region of the free-electron-to-heavy-hole continuum to be more clearly monitored. Furthermore, our samples all exhibit sharp luminescence lines typical of good optical-quality (In,Ga)As-GaAs quantum wells,^{12,13} increasing the likelihood of resolving additional exciton peaks. To our knowledge, very little experimental work has been reported on the formation of minibands in (In,Ga)As-GaAs superlattices. One exception is photoreflectance (PR) spectroscopy, at 77 and 300 K, which has been used to characterize two multiple well samples with well widths of 50 or 30 Å, and 100-Å barriers. From these PR data¹⁴

transitions at both the center and the edge of the minizone are inferred from the number of levels needed to fit the PR line shape, while also allowing the indium fraction and the well-to-barrier ratio to be adjusted. However, the data we present here is the first report of sharp excitonic features due to the $n = 1$ and 2 e -hh subbands, associated with the dispersion of the energy band structure in (In,Ga)As-GaAs strained-layer superlattices.

SAMPLE DETAILS AND EXPERIMENTAL TECHNIQUE

The (In,Ga)As superlattice samples we used in this study were all grown by molecular-beam epitaxy in a Varian modular Gen II machine. The layers were deposited on undoped (001) GaAs substrates, rotated at ~ 20 rpm. The growth rates of GaAs and (In,Ga)As were measured using the reflection high-energy electron diffraction (RHEED) oscillation technique on a GaAs monitor slice prior to the growth of the samples. Using this technique, the fluxes of indium and gallium were adjusted so that the nominal indium fraction in the alloy layers would be ~ 0.06 . The four samples used in this study were all deposited at a substrate temperature of $\sim 530^\circ\text{C}$. The nominal growth sequence was as follows: (a) a $1\text{-}\mu\text{m}$ GaAs buffer, (b) 20 periods of $50\text{-}\text{\AA}$ (In,Ga)As wells and GaAs barriers of either 200, 150, 100, or 50 \AA , and (c) a 200 \AA GaAs capping layer.

All the samples have been studied by x-ray diffraction (XRD).¹⁵ The average indium concentrations in the superlattices were obtained by simulation of the 004 double-crystal "rocking curve" and the extent of any relaxation by studying the asymmetric 115 reflection. The periods, d , were derived from the satellite positions close to the 004 peak on a powder diffractometer and the well and barrier widths were obtained by modeling their amplitudes and comparing with the measured values.¹⁶ No individual well and barrier thicknesses could be reliably determined for the $50\text{-}\text{\AA}$ well, 50 \AA barrier sample, since only the first-order satellites had measurable intensity and could indicate that the interfaces are poorer in this sample.¹⁷ We do not expect that any sample exceeds the critical thickness limit for the relaxation of the compressive strain in the (In,Ga)As and indeed there was no XRD evidence for relaxation in any of these samples. The measured values of alloy composition and well and barrier thickness are given in Table I. The XRD measurements are clearly somewhat different from the nomi-

nal values expected from the growth parameters. Consider first the composition of the alloy layers; typically the measured indium fractions are ~ 0.015 lower than the intended value. At these low compositions the InAs growth rate is extracted from our measurements of the GaAs and (In,Ga)As rates so that the uncertainty in determining such a low growth rate could produce an error in the absolute composition of $\pm 2\%$. The XRD measurements are therefore within the experimental limits we place on our growth data. Consider now the measurements of the SL period d , which are on average $\sim 7\%$ larger than the nominal thicknesses. Again, although this is somewhat larger than we might expect, these values are not outside the errors which may be introduced in the growth rate measurements. Finally, we look at the ratio of the well to barrier thickness. The XRD measurements suggest that an increase in the thickness of the (In,Ga)As (and not the GaAs) layers accounts for the increase in the SL period. We cannot explain this observation simply, based on our existing knowledge about the growth of (In,Ga)As on GaAs and this discrepancy is still under investigation.

Photoluminescence (PL) and photoluminescence excitation (PLE) spectra were recorded at $\sim 4\text{ K}$. The PL measurements were made using an Ar^+ pumped dye (styryl-9) laser, set above the GaAs band gap, at 8060 \AA , as the excitation source. The same dye laser provided the tunable source for the PLE measurements. In addition we performed circularly polarized PLE (PPLE) measurements¹⁸ in which the linearly polarized laser light was chopped by an oscillating stress plate to produce alternating σ^+ and σ^- excitation. The PPLE spectra were recorded at the peak of the luminescence signal, $e1\text{-}hh1$, selectively detecting changes in only one sense of the circularly polarized emission. We arranged the phase of the detection system so that a transition involving a heavy-hole state, which increases the PL signal, gave rise to peaks, whilst absorption from a light-hole state, which decreases the PL intensity, produced dips in the PPLE spectra. The PPLE data is an essential part of these investigations because it allows us to distinguish between heavy-hole and light-hole exciton transitions, thus eliminating some of the ambiguities otherwise associated with the assignment of the spectral features.

EXPERIMENTAL RESULTS AND DISCUSSION

We have recorded low temperature PL, PLE, and PPLE spectra on each of the four (In,Ga)As-GaAs SL

TABLE I. Comparison of the measured and calculated intersubband transitions using the values of indium concentration (x) and layer thicknesses determined by x-ray-diffraction techniques. The (In,Ga)As/GaAs dimensions are in \AA and the transition energies are in eV.

Sample structure		$(e1\text{-}hh1)\Gamma$		$(e1\text{-}lh1)\Gamma$		$(e1\text{-}hh2)\Gamma$		$(e1\text{-}hh2)\Pi$		$(e2\text{-}hh2)\Pi$	
(In,Ga)As/GaAs	x	Expt.	Calc.	Expt.	Calc.	Expt.	Calc.	Expt.	Calc.	Expt.	Calc.
65.2/202.7	0.044	1.4932	1.4954	1.5076	1.5058	1.5106	1.5082	1.5106	1.5083	1.5271	1.5269
68.2/146.0	0.041	1.4946	1.4954	1.5073	1.5055	1.5087	1.5102	1.5113	1.5112	1.5302	1.5307
57.7/104.1	0.0502	1.4924	1.4901	1.5055	1.5021	1.5096	1.5119	1.5139	1.5148	1.5372	1.5402

samples. We identify the samples by their nominal well-to-barrier thicknesses. All the data measured on the (50 Å)-(150 Å) sample are gathered together in Fig. 1. The PL spectrum of this sample is dominated by a single sharp emission line at 1.4896 eV with a measured linewidth of only 1.9 meV. The PLE spectrum recorded at the peak of the emission is shown as the upper curve in the same figure, while the polarized PLE data appears immediately below. The PPLE spectrum almost identically mimics the details of the unpolarized data with the exception of the sharp feature at 1.5023 eV which now appears as a prominent dip. This allows us to assign this peak to the $e1$ -lh1 exciton transition. The peak at 1.5147 eV appears in all our good optical quality (In,Ga)As-GaAs quantum well samples and can, from its energy position, be identified as the bulk GaAs free exciton, most probably arising from absorption in the buffer and substrate material.

In the energy region between the light-hole exciton and the GaAs band edge two additional peaks are clearly resolved, labeled in Fig. 1 as 1 and 2, both have heavy-hole character. Comparison of their measured energy positions with our envelope-function calculations leads us to assign these features to the symmetry-forbidden $e1$ -hh2 exciton transitions. Peak 1 corresponds to the transition at $q_z=0$, i.e., at the center of the mini-Brillouin zone, and is referred to as the $e1$ -hh2(Γ) exciton, while peak 2 is a direct transition at the 1D Brillouin zone edge, i.e., $q_z=\pi/d$, (d is the SL period) which we call $e1$ -hh2(Π). The observation of a splitting of the $e1$ -hh2 transition is a direct consequence of the subband dispersion and hence finite miniband widths, which gives rise to critical points in the energy band structure corresponding to the top and bottom of the minibands. The energy separation between this pair of transitions in the PLE spectrum provides a measurement of the sum of the electron and hole miniband widths.

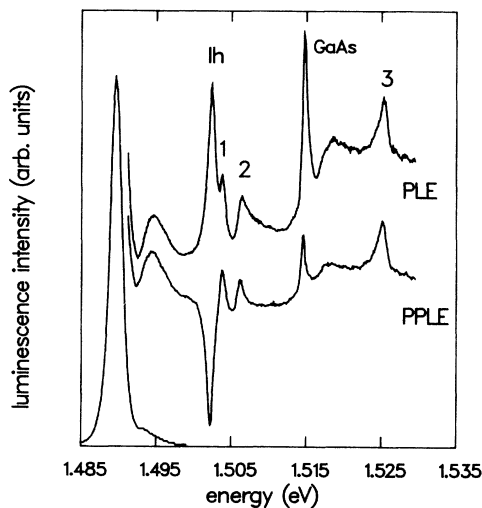


FIG. 1. Photoluminescence (PL), photoluminescence excitation (PLE), and polarized PLE (PPLE) spectra, recorded at 4 K, from the nominally (50 Å)-(150 Å) (In,Ga)As-GaAs superlattice sample.

The appearance of parity forbidden transitions ($\Delta n \neq 0$) in low-dimensional structures has been frequently reported by other authors.¹⁸⁻²⁰ The breakdown of the simple parity selection rule, $\Delta n = 0$, for quantum-well samples can arise from the presence of electric fields, or from the mixing of light- and heavy-hole subbands, or perhaps because of the presence of layer imperfections such as thickness variations, alloy fluctuations, or surface roughness. For the (In,Ga)As-GaAs superlattice samples studied here, we note that the hh2 state forms an unconfined miniband, a few meV above the heavy-hole valence-band step. Furthermore, because the confining barrier for the light holes is small, $\sim 2-3$ meV with our band-offset ratio, the lh1 subband is also unconfined, and has considerable overlap with the hh2 miniband. Therefore we suggest that in-plane mixing of the hh2 subband with the lh1 subband is the most probable intrinsic cause of the relaxation of the selection rules and the observation of $e1$ -hh2 excitons in our spectra. Both $e1$ -hh2 excitons are built from subbands where either one or other (but not both) of the effective masses are negative. This is in contrast to the reported saddle-point excitons in the GaAs-(Al,Ga)As superlattices,⁹⁻¹¹ in which the authors say the excitons are built from free carriers in the $n=1$ subbands at $q_z = \pi/d$, where both masses are negative. In this case, the solution to the effective-mass-like equation for the exciton has no bound states and the resonances are expected to be broad, as described by Kane.⁷ In our case ΔE_{e1} , the electron miniband width is greater than ΔE_{hh2} , the bandwidth of the $n=2$ heavy-hole state. Within a tight-binding framework, the effective mass at the subband extrema is proportional to $(\text{bandwidth})^{-1}$, so we expect, to a good first approximation, that $m_{e1}^* < m_{hh2}^*$, both at the zone center and at the zone edge. This means that the z component of the exciton reduced mass will be positive for the $e1$ -hh2(Γ) transition and negative for $e1$ -hh2(Π). The former is clearly able to support bound states (once it becomes allowed) while the latter again supports a resonance. This is borne out by our PLE data; peak 1 [$e1$ -hh2(Γ)] is a sharp feature with a line shape and half-width similar to the heavy-hole and light-hole excitons. Peak 2 [$e1$ -hh2(Π)], however, has an asymmetric shape and is noticeably broader.

A further prominent feature appears in the spectrum of Fig. 1, above the GaAs band edge, labeled as peak 3. This transition is reproduced as a peak in the PPLE spectrum, hence we associate this feature with an exciton transition having heavy-hole character. Comparison with our calculated band-to-band transitions leads us to assign peak 3 to the allowed $e2$ -hh2 exciton state. The dispersion of $n=2$ bands is such that the lowest-energy $e2$ -hh2 transition is at the minizone edge in the 1D band structure, hence we refer to peak 3 as $e2$ -hh2(Π). For samples of the structure and composition studied here, only the lowest-electron and heavy-hole states are below the top of the quantum wells. Therefore the $e2$ -hh2(Π) exciton state is built from electron and heavy-hole minibands which are both unconfined. This is to be compared with the $e1$ -hh2(Γ) and $e1$ -hh2(Π) exciton states which are derived from "delocalized," below-barrier electron states, and unconfined, above-barrier heavy-hole states.

We turn our attention now to the shape of the PLE spectrum (Fig. 1) between the heavy- and light-hole excitons. We observe a broad feature with a peak at about 1.4945 eV, reminiscent of similar structure we reported earlier²¹ on a (25 Å)-(100 Å) $\text{In}_x\text{Ga}_{1-x}\text{As}/\text{GaAs}$ MQW with $\sim 12\%$ indium in the alloy layers. This must, at least in part, be due to the excited states of the heavy-hole exciton and to the free-electron-to-heavy-hole continuum. However, the absorption strength is clearly enhanced over a simple stepwise density of states. This change in the oscillator strength stems from the existence of a dispersion relation in the SL miniband and from the presence of a saddle point at the minizone edge. Similar structure has previously been reported by Song and co-workers¹⁰ and also by Deveaud and co-workers,^{9,11} both groups having studied the GaAs-(Al,Ga)As system. We can make qualitative comparisons of our PLE data with the theoretically generated absorption curves of Chu and Chang,⁸ who have also considered the GaAs-(Al,Ga)As system. Their calculations take into account the presence of the M_1 singularity in the energy band structure, expanding the exciton wave functions over the whole Brillouin minizone. While the total integrated area of the absorption curve must remain the same, their generated data show a dramatic change in spectral shape in the region of the heavy-hole continuum, brought about by a redistribution of the oscillator strength due to the electron-hole Coulomb interaction within the miniband. The shape of the broad peaked structure in Fig. 3 of their data for a (80 Å)-(42 Å) GaAs-(Al_{0.25}Ga_{0.75})As SL compares rather favorably with our measurements on the (50 Å)-(150 Å) (In,Ga)As-GaAs SL. We account for this agreement simply by noting the similar size of the electron miniband widths for these structures, which we calculate to be 6.4 and 5.3 meV, respectively. Note that these widths are, in both cases, of the order of the heavy-hole exciton binding energy.^{22,23}

The PL and PLE data on all four samples studied are illustrated in Fig. 2. Nominally the samples all have the same (In,Ga)As well thickness and composition and barrier thicknesses of 200, 150, 100, and 50 Å. Consider first the PL spectra, shown as dashed curves. Splittings of the emission peaks of 0.7 and 1.1 meV are revealed for two of the samples, namely the (50 Å)-(200 Å) and (50 Å)-(100 Å) layers respectively. Splittings of the heavy-hole exciton peaks in these samples are also observed in the PLE spectra where, in both cases the measured energy positions exactly coincide with the PL lines. This is most probably brought about by some small inhomogeneity in the samples, of either the composition and/or layer thickness, which can produce exciton localization effects even in coupled quantum-well structures.²¹

The PLE spectra in Fig. 2 have all been recorded in two parts; first the detection was set to the peak of each luminescence line while scanning the excitation source to higher energy. Secondly, detection on the low-energy side of the emission was used to measure the position of the $e1\text{-hh}1$ exciton peak. Not shown in the figure are the PPLE spectra, which have also been recorded for each of the samples. In all cases the circularly polarized excitation experiment revealed similar data to that already dis-

cussed, and illustrated in Fig. 1, for the (50 Å)-(150 Å) sample. A prominent dip in each PPLE spectrum appeared at the position of the peak labeled as the light-hole exciton. All other features were identified as having heavy-hole character. Peaks 1, 2, and 3 are again observed in all but the sample with the thinnest barrier layers. Following the same procedure as before we ascribe these features as ($e1\text{-hh}2$) Γ , ($e1\text{-hh}2$)II, and ($e2\text{-hh}2$)II, respectively.

For a detailed comparison of the measured exciton positions with our calculations we refer to Table I. The calculations are made using the values of composition and well and barrier thickness determined by x-ray-diffraction techniques.¹⁵ We exclude the (50 Å)-(50 Å) sample from the comparison because of the limited structural information we have on this sample. While, as previously discussed, there may be some uncertainty associated with the values of well and barrier thickness as determined by analysis of the x-ray-diffraction data, we do not expect small adjustments to the layer thicknesses to alter our assignments of the spectral features. In fact, were we to assume the nominal values of L_z and L_b then a small change in the value of the GaAs deformation potential produces similar agreement between theory and experiment. The calculations assume that all the bands are parabolic and that the band-offset ratio for strained (In,Ga)As-GaAs electron-to-heavy-hole band gaps is 67:33. This choice of Q_c is still a matter of some controversy,²⁴ particularly for structures which incorporate

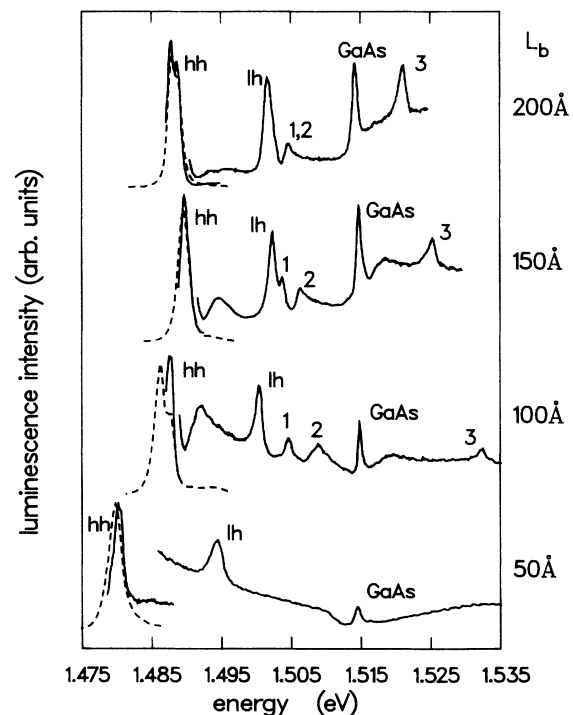


FIG. 2. Photoluminescence and photoluminescence excitation spectra, recorded at 4 K, of four (In,Ga)As-GaAs superlattices. The nominal barrier thickness of each sample is given in Å.

only a relatively small amount of indium into the well layers ($x < 0.08$), and we return to this point later in the discussion. The effects of the uniaxial and hydrostatic components of the strain on the band gap of the well material are included in the calculation. We adopt the value of the GaAs deformation potential ($a = -7.1$ eV) used by Gershoni and co-workers to fit optical data on both (In,Ga)As-InP (Ref. 25) and (In,Ga)As-GaAs (Ref. 26) quantum wells. All other details of the calculation can be found in Refs. 14 and 27. To make a comparison between the exciton positions measured experimentally and our calculated band-to-band transitions we assume a fixed value for the binding energy of all the exciton states of 6 meV. This is in line with experimentally determined values of the $e1$ -hh1 heavy-hole binding energy by ourselves²³ and by others²⁸ in this material system. The agreement with all the measured exciton transitions is excellent. In many cases the calculations are within 1 meV of the experiment and at worst the discrepancy is only ~ 3 meV.

Consider now the consequences of adopting a band-offset ratio of 40:60, as suggested by Menendez and co-workers,²⁹ on our interpretation of the PLE data. Using the same measurements of composition and layer thicknesses, as determined by x-ray-diffraction techniques, we have attempted to reassign the spectral features, allowing the GaAs deformation potential to vary between the value used by Gershoni and co-workers²⁶ ($a = -7.1$ eV), and Pan and co-workers¹⁴ ($a = -9.8$ eV), to fit optical spectra on (In,Ga)As-GaAs quantum-well structures. Following this procedure we are able to obtain a reasonable fit (within ~ 3 meV) to the positions of the $e1$ -hh1 and $e1$ -lh1 exciton states. The best fit to these transitions was in fact achieved with $a = -9.8$ eV. However, the energy positions of the $e1$ -hh2(Γ) and $e1$ -hh2(Π) transitions are much more sensitive to the choice of Q_c . Using this alternative parameter set the calculated energy positions of these excitons lie above the band gap of GaAs, for the samples studied here. Clearly, the spectral features we observe appear well below the GaAs exciton. Furthermore, we are not able to find alternative assignments for all the measured peaks which in a consistent way explain our observations as a function of barrier thickness.

The predicted evolution of all the transitions, both at the center and at the edge of the minizone, is best displayed as shown in Fig. 3. Each transition has been calculated as a function of GaAs barrier thickness, for a fixed value of (In,Ga)As well thickness and composition. For illustrative purposes we have chosen average values of both parameters, obtained by taking the mean of the x-ray diffraction results on the three well-characterized samples, i.e., an indium fraction of 0.045 and a well width of 64 Å. Studying Fig. 3 in relation to the PLE data provides us with a clear picture of the evolution of the minibands with decreasing barrier thickness. For example, it is immediately obvious that for the (50 Å)-(200 Å) sample we expect to resolve only one $e1$ -hh2 transition. This is because for a sample with these dimensions, it turns out that both the $e1$ and hh2 minibands have similar widths (2 meV), so that the calculated transition energies at the

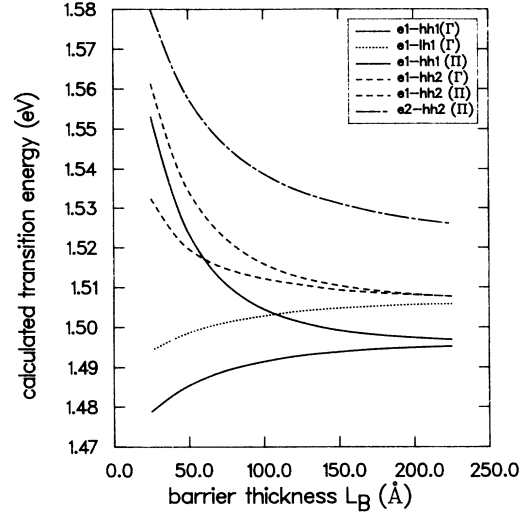


FIG. 3. Calculated band-to-band transitions as a function of GaAs barrier thickness, for a fixed (In,Ga)As well width of 64 Å and composition of 0.045. Transitions at the minizone center are labeled as Γ and those at the zone edge as Π . The calculations are made assuming a band-offset ratio of 67:33.

zone center and zone edge are precisely coincident (see Table I). Furthermore, it is quite apparent that we would not expect to observe peaks 1, 2, or 3 in the spectrum of the (50 Å)-(50 Å) sample. Peak 1 should appear in the same energy region of the spectrum as the GaAs exciton, while peaks 2 and 3 are predicted to be at a higher energy than investigated in these experiments.

In addition to the evolution of the exciton features with decreasing barrier thickness, already described above, we are able to monitor changes in the shape of the PLE spectra, in the region of the heavy-hole continuum states. For the sample with the thickest barriers, there is very little dispersion of the band structure in the growth direction, in fact this structure is a good approximation to an isolated multiple quantum well. The steplike continuum we observe in the PLE spectrum is therefore entirely consistent with the two-dimensional density of states we would anticipate. However, as the barrier thickness is reduced to 150 Å, the spectral shape in this region develops into a broad peak, which as already discussed is considerably enhanced over a stepwise density of states. Another decrease in GaAs thickness to 100 Å produces an even greater effect; there being a marked asymmetric broadening and further enhancement to the absorption strength. The evolution of this feature can be correlated with an increase in the dispersion of the superlattice band structure in the growth direction. In fact the changes in shape of the continuum states we observe, compare most favorably with the theoretically generated absorption curves of Chu and Chang,⁸ for GaAs-(Al,Ga)As samples with different barrier thicknesses. For the sample with the thinnest barriers the dispersion of the electron subband in the growth direction is considerably greater (~ 43 meV) than the binding energy of the heavy-hole exciton state. The resulting absorption spectrum for energies below the saddle point therefore tends towards bulk GaAs.

SUMMARY

We have used photoluminescence excitation spectroscopy to study the evolution of superlattice minibands in (In,Ga)As-GaAs structures with 50-Å wells and barrier layers between 200 and 50 Å. Comparing the measured exciton positions with envelope-function type calculations we are able to fit all the spectral features using a band-offset ratio of 67:33, the agreement is excellent. No consistent picture describing all the observations can be obtained by invoking a 40:60 ratio, which has been suggested²⁹ for samples with small indium fractions. The observed exciton peaks are consistent with theoretical predictions of $\Delta n = 0$ and $\Delta n \neq 0$ (i.e., $e1$ -hh2) intersubband transitions involving both "delocalized," below barrier subbands, and, "unconfined" minibands above the GaAs band edge. As the barrier thickness is decreased, we observe a splitting of the $e1$ -hh2 exciton peak, brought about by the increased dispersion in the growth direction,

which leads to different excitonic transition energies at the center of the superlattice minizone and at the zone edge. Furthermore, as the miniband dispersion is increased, we observe a dramatic change in the shape of the PLE spectra in the region of the free-electron-to-heavy-hole continuum. A significant enhancement of the absorption strength is noted, brought about by a redistribution of the oscillator strength due to the Coulomb interaction between electrons and holes in the miniband. The most significant effects occur when the electron miniband width is of the order of the heavy-hole exciton binding energy.

ACKNOWLEDGMENTS

We are indebted to Paul Fewster for providing details of the x-ray-diffraction analysis and thank John Orton for many valuable discussions during the course of this work.

*Permanent address: FOM, Institute for Atomic and Molecular Physics, KruisLaan 407, 1098 SJ Amsterdam, The Netherlands.

¹R. Dingle, *Festkörperprobleme* **15**, 21 (1975).

²C. Weisbuch, in *Semiconductors and Semimetals*, edited by R. Dingle (Academic, San Diego, 1987), Vol. 24, p. 1.

³G. Bastard, *Phys. Rev. B* **24**, 5693 (1981).

⁴G. Bastard and J. A. Brum, *IEEE J. Quantum Electron.* **QE-22**, 1625 (1986).

⁵J. C. Phillips, *Phys. Rev.* **136**, A1705 (1964).

⁶B. Velicky and J. Sak, *Phys. Status Solidi* **16**, 147 (1966).

⁷E. O. Kane, *Phys. Rev.* **180**, 852 (1969).

⁸H. Chu and Y.-C. Chang, *Phys. Rev. B* **36**, 2946 (1987).

⁹B. Deveaud, A. Chomette, F. Clerot, A. Regreny, J. C. Maan, R. Romestain, G. Bastard, H. Chu, and Y.-C. Chang, *Superlatt. Microstruct.* **6**, 183 (1989).

¹⁰J. Song, P. S. Jung, Y. S. Yoon, H. Chu, Y.-C. Chang, and C. W. Tu, *Phys. Rev. B* **39**, 5562 (1989).

¹¹B. Deveaud, A. Chomette, F. Clerot, A. Regreny, J. C. Maan, R. Romestain, G. Bastard, H. Chu, and Y.-C. Chang, *Phys. Rev. B* **40**, 5802 (1989).

¹²D. C. Bertolet, J.-K. Hsu, S. H. Jones, and K. M. Lau, *Appl. Phys. Lett.* **52**, 293 (1988).

¹³D. C. Bertolet, J.-K. Hsu, K. M. Lau, E. S. Koteles, and D. Owens, *J. Appl. Phys.* **64**, 6562 (1988).

¹⁴S. H. Pan, H. Shen, Z. Hang, F. H. Pollak, W. Zhuang, Q. Xu, A. P. Roth, R. A. Masut, C. Lacelle, and D. Morris, *Phys. Rev. B* **38**, 3375 (1988).

¹⁵P. F. Fewster and N. L. Andrew (private communication).

¹⁶P. F. Fewster, *Philips J. Res.* **41**, 268 (1986).

¹⁷P. F. Fewster, *J. Appl. Cryst.* **21**, 524 (1988).

¹⁸C. Weisbuch, R. C. Miller, R. Dingle, A. C. Gossard, and W. Wiegman, *Solid State Commun.* **37**, 219 (1980).

¹⁹Y. C. Chang and J. N. Schulman, *Phys. Rev. B* **31**, 2069 (1985); *Appl. Phys. Lett.* **43**, 536 (1983).

²⁰V. K. Reddy, G. Ji, T. Henderson, H. Morkoc, and J. N. Schulman, *J. Appl. Phys.* **62**, 145 (1987).

²¹K. J. Moore, G. Duggan, K. Woodbridge, and C. Roberts, *Phys. Rev. B* **41**, 1095 (1990).

²²P. Dawson, K. J. Moore, G. Duggan, H. I. Ralph, and C. T. B. Foxon, *Phys. Rev. B* **34**, 6007 (1986).

²³K. J. Moore, G. Duggan, K. Woodbridge, and C. Roberts, *Phys. Rev. B* **41**, 1090 (1990).

²⁴M. J. Joyce, M. J. Johnson, M. Gal, and B. F. Usher, *Phys. Rev. B* **38**, 10978 (1988).

²⁵D. Gershoni, H. Temkin, M. B. Panish, and R. A. Hamm, *Phys. Rev. B* **39**, 5531 (1989).

²⁶D. Gershoni, J. M. Vandenberg, S. N. G. Chu, H. Temkin, T. Tanbun-Ek, and R. A. Logan, *Phys. Rev. B* **40**, 10017 (1989).

²⁷K. J. Moore, *Spectroscopy of Semiconductor Microstructures*, Vol. 206 of *NATO Advanced Study Institute, Series B: Physics*, edited by G. Fasol, A. Fasolino, and P. Lugli (Plenum, New York, 1989).

²⁸N. J. Pulsford and R. J. Nicholas (unpublished).

²⁹J. Menendez, A. Pinczuk, D. J. Werder, S. K. Sputz, R. C. Miller, D. L. Sivco, and A. Y. Cho, *Phys. Rev. B* **36**, 8165 (1987).